Constraints on electromagnetic form factors of sub-GeV dark matter from the cosmic microwave background anisotropy

Gaetano Lambiase,[1,2] Subhendra Mohanty,[3] Akhilesh Nautiyal,[4] and Soumya Rao[3]

[1]*Dipartimento di Fisica E.R. Caianiello, Universit degli Studi di Salerno, Via Giovanni Paolo II, 132–84084 Fisciano (SA), Italy*

[2]*INFN, Gruppo Collegato di Salerno, Via G. Paolo II, 84084-Fisciano (Salern), Italy*

[3]*Theory Division, Physical Research Laboratory, Navrangpura, Ahmedabad 380 009, India*

[4]*Department of Physics, Malaviya National Institute of Technology, JLN Marg, Jaipur 302017, India*

(Received 19 February 2021; accepted 22 June 2021; published 16 July 2021)

We consider dark matter which has nonzero electromagnetic form factors like electric/magnetic dipole moments and anapole moment for fermionic dark matter and Rayleigh form factor for scalar dark matter. We consider dark matter mass $m_\chi > \mathcal{O}(\mathrm{MeV})$ and put constraints on their mass and electromagnetic couplings from cosmic microwave background (CMB) and large scale structure (LSS) observations. Fermionic dark matter with nonzero electromagnetic form factors can annihilate to e^+e^- and scalar dark matter can annihilate to 2γ at the time of recombination and distort the CMB. We analyze dark matter with multipole moments with Planck and baryon acoustic oscillations (BAO) observations. We find upper bounds on anapole moment $g_A < 7.163 \times 10^3\ \mathrm{GeV}^{-2}$, electric dipole moment $\mathcal{D} < 7.978 \times 10^{-9}\ e\,\mathrm{cm}$, magnetic dipole moment $\mu < 2.959 \times 10^{-7}\mu_B$, and the bound on Rayleigh form factor of dark matter is $g_4/\Lambda_4^2 < 1.085 \times 10^{-2}\ \mathrm{GeV}^{-2}$ with 95% C.L.

DOI: 10.1103/PhysRevD.104.023519

I. INTRODUCTION

It is well accepted that formation of large scale structures and the rotation curves of galaxies require an extra dark matter (DM) component beyond the known particles of the standard model. The particle properties of this dark matter are, however, completely unknown. Direct detection experiments, which rely on nuclear scattering, have ruled out a large parameter space. But, these techniques are not efficient in measuring dark matter of sub-GeV mass [1,2]. To measure sub-GeV mass dark matter a suitable method is scattering electrons from heavy atoms [3–8]. Dark matter with nonzero electric or magnetic dipole moments [9–11] or anapole moment [12,13] can be very effective in scattering electrons. The electromagnetic form factors can be viewed as effective operators [14–17], which arise by integrating out the heavy particles in an ultraviolet complete theory [18].

The electromagnetic couplings of dark matter can be constrained from cosmic microwave background and large scale structure observations. The electric and magnetic dipole moment vertex can give rise to dark matter-baryon coupling. For heavy dark matter ($\sim$100 GeV) the baryon drag on the dark matter will show up in structure formation and cosmic microwave background (CMB) [10]. Light dark matter $\mathcal{O}(\mathrm{MeV})$ will annihilate to radiation and lower the effective neutrino number (N_{eff}) [19–21].

In this paper we will analyze the effect of light dark matter with electromagnetic form factors on CMB anisotropy and polarization from dark matter annihilation to e^+e^- or photons close to recombination era, $z \sim 1100$. The effects of annihilating dark matter on CMB are studied in [22–26]. Production of relativistic e^+, e^- heats up the thermal gas and ionizes the neutral hydrogen, which increases the free electron fraction. Due to this increased free electron fraction there is a broadening of the last scattering surface and suppression of CMB temperature anisotropy. The low-l correlations between polarization fluctuations are also enhanced due to increased freeze-out value of the ionization fraction of the universe after recombination. These effects on CMB are significant and can be used to put constraints on thermal averaged annihilation cross section $\langle\sigma v\rangle$. Planck-2018 reports $\langle\sigma v\rangle < (3.2 \times 10^{-28}/f) \times (M_{\mathrm{DM}}/(\mathrm{GeV}/c^2))\ \mathrm{cm}^3/\mathrm{s}$ for velocity independent thermal average cross section [27]. Here f is the fraction of energy injected to the intergalactic medium (IGM) by annihilating dark matter. Forecasts for upcoming CMB experiments such as AdvACTPol, AliCPT, CLASS, Simons Array, Simons Observatory, and SPT-3G have been studied by [28] in detecting decaying/annihilating dark matter, and it is found that $\langle\sigma v\rangle \sim (10^{-29}/f) \times (M_{\rm DM}/({\rm GeV}/c^2))\ {\rm cm}^3/{\rm s}$.

The annihilation $\chi\chi \to e^+e^-$ occurs with one dipole or anapole vertex and the annihilation cross sections are quadratic in dipole or anapole moments. For fermionic dark matter the $\chi\chi \to \gamma\gamma$ annihilation cross section is quartic in dipole moments and the bounds from this process are much weaker [29] than the ones we derive in this paper from CMB. For anapole dark matter the cross section for the process $\chi\chi \to \gamma\gamma$ is zero [12]. Scalar dark matter can have dimension-6 Rayleigh operator vertex with two-photons. For such Rayleigh dark matter the leading order contribution to annihilation will be from the $\phi\phi \to \gamma\gamma$ process which can distort the CMB near recombination and from this we put bounds on the dark-matter photon Rayleigh coupling.

This paper is organized as follows. In Sec. II we list the electromagnetic form factors of dark matter which we shall constrain from CMB data. In Sec. III we discuss the physics of recombination and the effect of dark matter annihilation on the CMB. In Sec. IV we compare the CMB analysis with data from Planck and BAO and using COSMOMC we put constraints on the dark matter form factors. In Sec. V we compare our bounds with earlier results and from other experiments, and in Sec. VI we summarize our results and give our conclusions.

II. ELECTROMAGNETIC FORM FACTORS OF DARK MATTER

Spin-1/2 dark matter can have the following electromagnetic form factors. These are the magnetic moment described by the dimension-5 operators,

$$\mathcal{L}_{\rm magnetic} = \frac{g_1}{\Lambda_1}\bar{\chi}\sigma^{\mu\nu}\chi F_{\mu\nu}, \tag{1}$$

where g_1 is a dimensionless coupling and Λ_1 is the mass scale of the particles in the loop which generate the dipole moment. The magnetic moment of Dirac fermions is $\mu = 2g_1/\Lambda_1$ and the operator (1) is zero for Majorana fermions.

Similarly electric dipole operator is of dimension-5,

$$\mathcal{L}_{\rm electric} = \frac{g_2}{\Lambda_2} i\bar{\chi}\sigma^{\mu\nu}\gamma_5\chi F_{\mu\nu}, \tag{2}$$

where the electric dipole moment of Dirac fermions is $\mathcal{D} = 2g_2/\Lambda_2$ and the operator (2) is zero for Majorana fermions.

Finally the anapole moment is a dimension-6 operator

$$\mathcal{L}_{\rm anapole} = \frac{g_3}{\Lambda_3^2} i\bar{\chi}\gamma^\mu\gamma_5\chi\partial^\nu F_{\mu\nu}. \tag{3}$$

This operator is nonzero for Dirac as well as Majorana fermions and the coefficient $g_A = g_3/(\Lambda_3^2)$ is called the anapole moment of χ.

Stringent bounds on sub-GeV mass dark matter are put from the observation of $\chi e^- \to \chi e^-$ scattering [3] in direct detection experiments like Xenon-10 [4], DarkSide [5] and Xenon-1T [6].

Using the experimental limits on dark matter electron scattering from Xenon-10, Xenon-1T and DarkSide bound on the electric dipole, magnetic dipole and anapole form factors of dark matter have been put in Refs. [7,8].

Real and complex scalar dark matter can have interaction with two-photons by dimension-6 Rayleigh operator

$$\mathcal{L}_{2\phi2\gamma} = \frac{g_4}{\Lambda_4^2}\phi^*\phi F_{\mu\nu}F^{\mu\nu}. \tag{4}$$

These will contribute to $\phi\phi \to \gamma\gamma$ annihilations which can be constrained from CMB [17]. In the absence of CP violation the $\tilde{F}F$ operator does not arise. The annihilation $\phi\phi \to \gamma\gamma$ takes place via s-wave in the leading order and cross section $\sigma(\phi\phi \to \gamma\gamma)v \simeq (g_4^2)m_\phi^2/\Lambda_4^4$ [17]. Bounds on the operator (4) from Xenon1T [6] and gamma ray searches from dwarf spheroidal satellites (dSphs) [30] and halo of the Milky Way [31] by Fermi-LAT are obtained in Ref. [17] for dark matter with mass larger than $\mathcal{O}(\rm GeV)$.

III. THERMAL HISTORY OF THE UNIVERSE WITH ANNIHILATING DARK MATTER

Recombination occurs around $z = 1100$ when electrons and protons combine together to form neutral hydrogen. If the annihilation cross section of dark matter particles is sufficiently large, it can modify the history of recombination and hence can leave a clear imprint on CMB power spectrum. The shower of particles produced due to annihilation can interact with the thermal gas in three different ways. (i) The annihilation products can ionize the thermal gas, (ii) can induce induce Lyman-α excitation of the hydrogen that will cause more electrons in the $n = 2$ state and hence increase the ionization rate and (iii) can heat the plasma. Due to the first two effects the evolution of free electron fraction χ_e changes and the last effect changes the temperature of baryons. The equation governing the evolution of the ionization fraction in the presence of annihilating particles is given as

$$\frac{d\chi_e}{dt} = \frac{1}{(1+z)H(z)}[R_s(z) - I_s(z) - I_X(z)]. \tag{5}$$

Here R_s is the standard recombination rate, I_s is the ionization rate due to standard sources and I_X is the ionization rate due to annihilating dark matter particles. The computation of standard recombination rate was done in [32–34] and it is described as

$$[R_s(z) - I_s(z)] = C \times [\chi_e^2 n_H \alpha_B - \beta_B(1-\chi_e)e^{-h_p\nu_{2s}/k_BT_b}]. \tag{6}$$

Here n_H is the number density of hydrogen nuclei, α_B and β_B are the effective recombination and photoionization rates for principle quantum numbers ≥ 2 in Case B recombination, ν_{2s} is the frequency of the $2s$ level from the ground state and T_b is the temperature of the baryon gas. The factor C appearing in Eq. (6) is given by

$$C = \frac{[1 + K\Lambda_{2s1s} n_H(1-\chi_e)]}{[1 + K\Lambda_{2s1s} n_H(1-\chi_e) + K\beta_B n_H(1-\chi_e)]}. \quad (7)$$

Here Λ_{1s2s} is the decay rate of the metastable $2s$ level, $n_H(1-\chi_e)$ is the number of neutral ground state H atoms and $K = \frac{\lambda_\alpha^3}{8\pi H(z)}$, where $H(z)$ is the Hubble expansion rate at redshift z and λ_α is the wavelength of the Ly-α transition from the $2p$ level to the $1s$ level.

The term I_X appearing in Eq. (5) represents the evolution of free electron density due to nonstandard sources. In our case it is due to annihilation of dark matter during recombination, which increases the ionization rate in two ways: (i) by direction ionization from the ground state and (ii) by additional Ly-α photons, which boosts the population at $n = 2$ increasing the rate of photoionization by CMB. Hence, the ionization rate I_X due to dark matter annihilation is expressed as

$$I_X(z) = I_{Xi}(z) + I_{X\alpha}(z). \quad (8)$$

Here $I_{Xi}(z)$ represents the ionization rate due to ionizing photons and $I_{X\alpha}$ represents the ionization rate due to Ly-α photons.

The rate of energy release $\frac{dE}{dt}$ per unit volume by a relic self-annihilating dark matter particle can be expressed in terms of its thermally averaged annihilation cross section $\langle\sigma v\rangle$ and mass m_χ as

$$\frac{dE}{dt} = 2g\rho_c^2 c^2 \Omega_{\mathrm{DM}}^2 (1+z)^6 f(z) \frac{\langle\sigma v\rangle}{m_\chi}, \quad (9)$$

where Ω_{DM} is the dark matter density parameter, ρ_c is the critical density today, g is degeneracy factor $1/2$ for Majorana fermions and $1/4$ for Dirac fermions, and $f(z)$ is the fraction of energy absorbed by the CMB plasma, which is $O(1)$ factor and depends on redshift. A detailed calculation of redshift dependence of $f(z)$ for various annihilation channels is done in [25,35–38] using generalized parametrizations or principle components. It is shown in [26,39,40] that the redshift dependence of $f(z)$ can be ignored up to a first approximation, since current CMB data are sensitive to energy injection over a relatively narrow range of redshift, typically $z \sim 1000 - 600$. Hence $f(z)$ can be replace with a constant f, which we take as 1 for our analysis. Here we use "on-the-spot" approximation, which assumes that the energy released due to dark matter annihilation is absorbed by IGM locally [24,41,42].

The terms appearing on the right-hand side of Eq. (8) are related to the rate of energy release as

$$I_{Xi} = C\chi_i \frac{[dE/dt]}{n_H(z) E_i} \quad (10)$$

$$I_{X\alpha} = (1-C)\chi_\alpha \frac{[dE/dt]}{n_H(z) E_\alpha}. \quad (11)$$

Here E_i is the average ionization energy per baryon, E_α is the difference in binding energy between the $1s$ and $2p$ energy levels of a hydrogen atom, n_H is the number density of hydrogen nuclei, and χ_i and χ_α represent the fraction of energy going ionization and Ly-α photons respectively, which can be expressed in terms of free electron fraction as $\chi_i = \chi_\alpha = (1-\chi_e)/3$ [22].

A fraction of energy released by annihilating dark matter particles also goes into heating the baryon gas, which modifies the evolution equation for the matter temperature T_b by contributing one extra term K_h as

$$(1+z)\frac{dT_b}{dz} = \frac{8\sigma_T a_R T_{\mathrm{CMB}}^4}{3m_e c H(z)} \frac{\chi_e}{1 + f_{He} + \chi_e}(T_b - T_{\mathrm{CMB}}) - \frac{2}{3k_B H(z)} \frac{k_h}{1 + f_{He} + \chi_e} + 2T_b. \quad (12)$$

Here the nonstandard term K_h arising due to annihilating dark matter is given in terms of rate of energy release as

$$K_h = \chi_h \frac{(dE/dt)}{n_H(z)}, \quad (13)$$

with $\chi_h = (1 + 2\chi_e)/3$ being the fraction of energy going into heat.

In this work we consider annihilating dark matter with electromagnetic form factors. We will now obtain the energy deposition rate for dark matter with anapole moment, electric dipole moment and magnetic dipole moment. One can define a quantity p_{ann} that depends on the properties of dark matter particles as

$$p_{\mathrm{ann}} = f \frac{\langle\sigma v\rangle}{m_\chi}. \quad (14)$$

The current constraint on p_{ann} with velocity independent $\langle\sigma v\rangle$ is $1.795 \times 10^{-7}\ \mathrm{m^3\,s^{-1}\,kg^{-1}}$ 95% C.L. from Planck-2018 [27]. In our analysis we will use various electromagnetic form factors and mass of the dark matter as our model parameters rather than p_{ann}. Hence we will express energy deposition rate in terms of these parameters for annihilating dark matter with anapole and dipole moments.

A. Dark matter with anapole moment

The annihilation cross section for dark matter with anapole moment is given as [12]

$$\langle\sigma v\rangle_{\chi\chi\to e^+e^-} = \frac{2g_A^2\alpha m_\chi^2}{3}v_{\rm rel}^2, \tag{15}$$

where $\alpha = e^2/(4\pi)$ and $v_{\rm rel}$ is average relative velocity between the annihilating dark matter particles in the center of mass frame. The thermally averaged velocity can be expressed in terms of temperature by $\frac{1}{2}(\frac{1}{2}m_\chi)\langle v_{\rm rel}^2\rangle = \frac{3}{2}T$. Hence the cross section (15) can be expressed in terms of temperature as

$$\langle\sigma v\rangle_{\chi\chi\to e^+e^-} = 4g_A^2\alpha m_\chi^2\left(\frac{T}{m_\chi}\right). \tag{16}$$

After decoupling the temperature of the dark matter behaves as $T \propto (1+z)^2$. Assuming the decoupling temperature of the dark matter T_d of the order of $\frac{m_\chi}{10}$ we get

$$T = T_d\frac{(1+z)^2}{(1+z_d)^2} = T_d\frac{T_0^2}{T_{\gamma d}^2}(1+z)^2 = \frac{10T_0^2}{m_\chi}(1+z)^2. \tag{17}$$

Here z_d and $T_{\gamma d}$ are the redshift of dark matter decoupling and the temperature of photons at that redshift respectively, which is the same as T_d. T_0 is the current temperature of CMB. Using Eq. (17) the annihilation cross section (16) becomes

$$\langle\sigma v\rangle_{\chi\chi\to e^+e^-} = 40g_A^2\alpha T_0^2(1+z)^2. \tag{18}$$

Hence using Eqs. (18) and (14) we can obtain the expression for $p_{\rm ann}$ as

$$p_{\rm ann} = \frac{40g_A^2\alpha T_0^2}{m_\chi}(1+z)^2. \tag{19}$$

As mentioned earlier we will choose $f \sim 1$ here. Since $p_{\rm ann}$ is velocity dependent, the rate of energy release given by Eq. (9) will be

$$\frac{dE}{dt} = \rho_c^2c^2\Omega_{\rm DM}^2\frac{40g_A^2\alpha T_0^2}{m_\chi}(1+z)^8. \tag{20}$$

Here the redshift dependence of the energy deposition rate is modified as compared to (9).

B. Dark matter with electric dipole moment

For DM with electric dipole moment the annihilation cross section is given by [11]

$$\langle\sigma v\rangle_{\chi\chi\to e^+e^-} = \frac{\alpha\mathcal{D}^2}{12}v_{\rm rel}^2, \tag{21}$$

where $v_{\rm rel}$ is the relative velocity of two annihilating weakly interacting massive particles. For thermal averaged cross section $T = m_\chi\langle v_{\rm rel}^2\rangle/3$. So the annihilation cross section for dark matter can be expressed in terms of temperature as

$$\langle\sigma v\rangle_{\chi\chi\to e^+e^-} = \frac{\alpha\mathcal{D}^2}{4}\left(\frac{T}{m_\chi}\right). \tag{22}$$

Assuming $T_d \sim \frac{m_\chi}{10}$ and using Eq. (17) for temperature of the dark matter the annihilation cross section for dark matter with electric dipole moment becomes

$$\langle\sigma v\rangle_{\chi\chi\to e^+e^-} = \frac{5\alpha\mathcal{D}^2T_0^2}{2m_\chi^2}(1+z)^2. \tag{23}$$

Hence using (14) we get

$$p_{\rm ann} = \frac{5\alpha\mathcal{D}^2T_0^2}{2m_\chi^3}(1+z)^2. \tag{24}$$

In this case the energy deposition rate will be

$$\frac{dE}{dt} = \frac{1}{2}\rho_c^2c^2\Omega_{\rm DM}^2\frac{5\alpha\mathcal{D}^2T_0^2}{2m_\chi^3}(1+z)^8. \tag{25}$$

Here also the redshift dependence is modified as compared to (9), since the thermally averaged cross section is velocity dependent.

C. Dark matter with magnetic dipole moment

For dark matter with magnetic dipole moment the annihilation cross section is given as [11]

$$\langle\sigma v\rangle_{\chi\chi\to e^+e^-} = \alpha\mu^2, \tag{26}$$

and hence

$$p_{\rm ann} = \frac{\alpha\mu^2}{m_\chi}. \tag{27}$$

Here the annihilation cross section does not depend on the velocity of dark matter so the energy deposition rate will be

$$\frac{dE}{dt} = \frac{1}{2}\rho_c^2c^2\Omega_{\rm DM}^2\frac{\alpha\mu^2}{m_\chi}(1+z)^6, \tag{28}$$

which has the same redshift dependence as in Eq. (9).

D. Rayleigh dark matter

For scalar dark matter with Rayleigh coupling (4) the annihilation cross section is given by [17]

TABLE I. Priors on input parameters for annihilating dark matter.

Type of dark matter coupling	Priors	
Anapole	$5.0 < \ln(10^9(g_A/GeV^{-2})) < 40$	$-3.0 < \log_{10}(m_\chi/GeV) < 2.0$
Electric dipole	$-5.0 < \ln(10^{18}(\mathcal{D}/(e-cm)) < 40$	$-3.0 < \log_{10}(m_\chi/GeV) < 2.0$
Magnetic dipole	$-10.0 < \ln(10^9(\mu/\mu_B)) < 15.0$	$-3.0 < \log_{10}(m_\chi/GeV) < 2.0$
Rayleigh coupling	$-10.0 < \ln(10^9 g_4/(\Lambda_4^2 GeV^{-2})) < 20.0$	$-12.0 < \log_{10}(m_\chi/GeV) < 2.0$

TABLE II. Planck-2018 and BAO constraints on anapole momentum and mass of the dark matter with the other six parameters of ΛCDM.

Parameter	68% limits	95% limits	99% limits
$\Omega_b h^2$	0.02243 ± 0.00013	$0.02243^{+0.00026}_{-0.00026}$	$0.02243^{+0.00034}_{-0.00034}$
$\Omega_c h^2$	0.11917 ± 0.00090	$0.1192^{+0.0018}_{-0.0018}$	$0.1192^{+0.0024}_{-0.0023}$
τ	0.0567 ± 0.0072	$0.057^{+0.015}_{-0.014}$	$0.057^{+0.020}_{-0.018}$
$\ln(10^9(g_A/GeV^{-2}))$	<22.6	<29.6	<31.9
$\log_{10}(m_\chi/GeV)$	…	…	…
$\ln(10^{10}A_s)$	3.048 ± 0.014	$3.048^{+0.029}_{-0.028}$	$3.048^{+0.039}_{-0.036}$
n_s	0.9670 ± 0.0037	$0.9670^{+0.0073}_{-0.0073}$	$0.9670^{+0.0097}_{-0.0096}$
H_0	67.73 ± 0.41	$67.73^{+0.81}_{-0.80}$	$67.7^{+1.1}_{-1.1}$

$$\langle\sigma v\rangle_{\phi\phi\to\gamma\gamma} = \frac{(g_4^2)m_\phi^2}{\Lambda_4^4}, \tag{29}$$

and hence

$$p_{\rm ann} = \frac{(g_4^2)m_\phi}{\Lambda_4^4}. \tag{30}$$

Here again the annihilation cross section is independent of the velocity of dark matter, so the energy deposition rate will be the same as (9):

$$\frac{dE}{dt} = \frac{1}{2}\rho_c^2 c^2 \Omega_{\rm DM}^2 \frac{(g_4^2)m_\phi}{\Lambda_4^4}(1+z)^6. \tag{31}$$

IV. CMB CONSTRAINTS ON VARIOUS MULTIPOLE MOMENTS OF DARK MATTER

As mentioned earlier annihilating dark matter increases the ionization fraction during recombination and heats the plasma. Hence the evolution equations of free electron fraction and matter temperature get modified as given by Eqs. (5) and (12) respectively. The nonstandard ionization rate I_X to compute free electron fraction can be obtained using Eq. (8) along with Eqs. (10) and (11). We use these equations along with energy deposition rates (20), (25), (28) and (31) for dark matter with anapole moment, electric dipole moment and magnetic dipole moment, and Rayleigh coupling to modify RECFAST routine [34] in CAMB [43]. We have also checked our

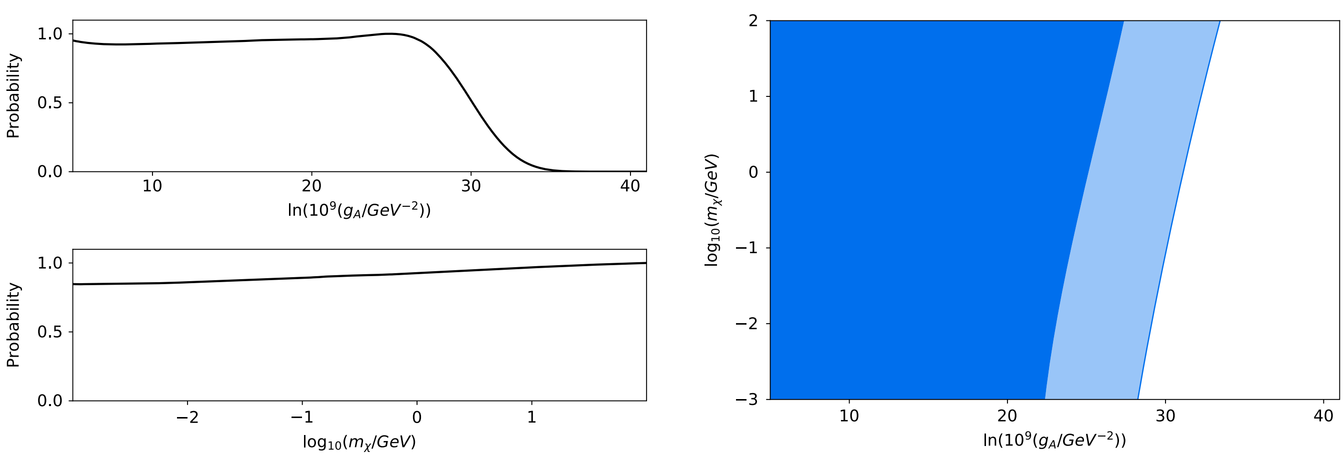

(a) Marginalized constraints

(b) Joint 68% CL and 95%CL constraints

FIG. 1. Constraints for anapole moment and mass of the dark matter using Planck-2018 and BAO data.

TABLE III. Planck-2018 and BAO constraints on electric dipole momentum and mass of the dark matter with the other six parameters of ΛCDM.

Parameter	68% limits	95% limits	99% limits
$\Omega_b h^2$	0.02244 ± 0.00014	$0.02244^{+0.00027}_{-0.00026}$	$0.02244^{+0.00036}_{-0.00034}$
$\Omega_c h^2$	0.11921 ± 0.00091	$0.1192^{+0.0018}_{-0.0018}$	$0.1192^{+0.0024}_{-0.0024}$
τ	0.0565 ± 0.0073	$0.056^{+0.015}_{-0.014}$	$0.056^{+0.020}_{-0.018}$
$\ln(10^{18}(\mathcal{D}/(e-cm)))$	<12.9	<22.8	<26.7
$\log_{10}(m_\chi/GeV)$	>-0.963	⋯	⋯
$\ln(10^{10}A_s)$	3.048 ± 0.014	$3.048^{+0.029}_{-0.028}$	$3.048^{+0.039}_{-0.037}$
n_s	0.9670 ± 0.0037	$0.9670^{+0.0071}_{-0.0073}$	$0.9670^{+0.0093}_{-0.0097}$
H_0	67.72 ± 0.41	$67.72^{+0.82}_{-0.79}$	$67.7^{+1.1}_{-1.0}$

analysis using CosmoRec [44] and HyRec [40,45] code instead of RECFAST, and we found similar results. With this we obtain modified theoretical angular power spectra, which can be used to compute the bounds on various electromagnetic form factors and mass of the dark matter from Planck-2018 data using COSMOMC [46]. The priors for the multipole moments and mass of the dark matter are given in Table I. All these priors are sampled logarithmically to cover a larger range for the new parameters. We also vary the other six parameters of ΛCDM model with priors given in [47]. We have imposed flat priors for all parameters.

We use the lower bound for the mass of dark matter with anapole moment, and electric and magnetic dipole moment as 1 MeV since the annihilation channel for this case is $\chi\chi \to e^+e^-$. However, in case of scalar dark matter with Rayleigh coupling [17], the dark matter annihilates to photons having energy around 1 eV during recombination, which is used as the lower bound for mass of Rayleigh dark matter. We also use BAO and Pantheon data along with Planck-2018 observations for our analysis. We perform MCMC convergence diagnostic tests on four chains using the Gelman and Rubin "variance of mean"/"mean of chain variance" R-1 statistics for each parameter.

The constraints obtained for anapole moment and mass of the dark matter along with other six parameters of ΛCDM model are shown in Table II. Figure 1 represents the marginalized constraints on anapole moment and mass of the dark matter along with joint 68% C.L. and 95% C.L. constraints on both the parameters from Planck-2018 and BAO data.

It can be seen from Table II that

$$g_A < 7.163 \times 10^3 \ \mathrm{GeV}^{-2} \quad 95\% \ \mathrm{C.L.} \qquad (32)$$

The constraints obtained using Planck-2018 and BAO data on electric dipole moment and the mass of the dark matter along with the other six parameters of the ΛCDM model are listed in Table III. Figure 2 depicts the marginalized constraints on electric dipole moment and mass of the dark matter and with joint 68% C.L. and 95% C.L. constraints on both the parameters from Planck-2018 and BAO data.

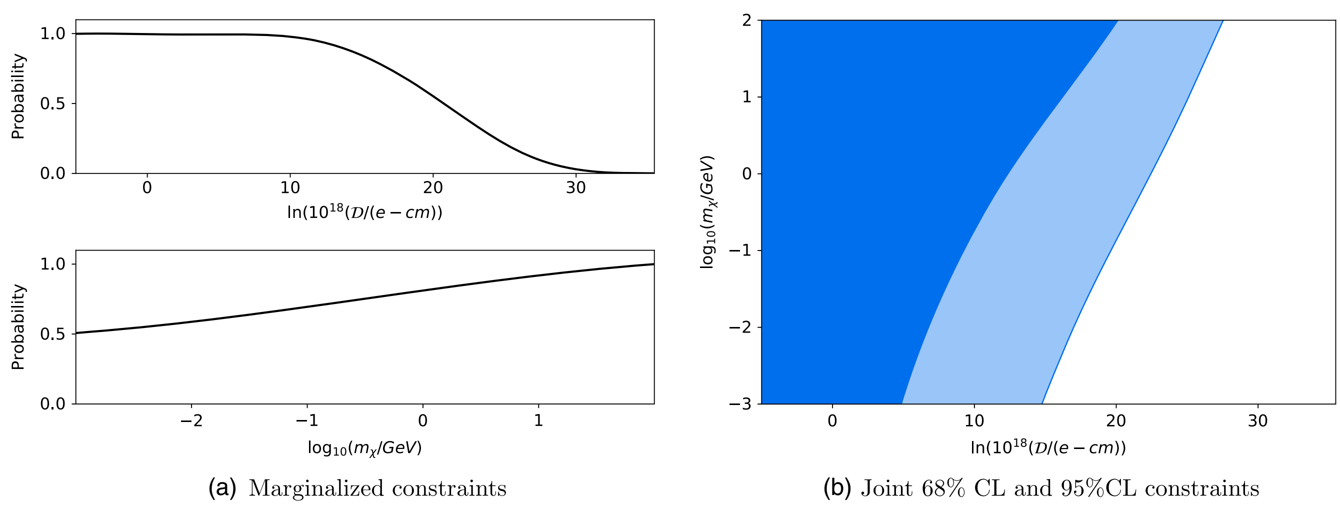

FIG. 2. Constraints for electric dipole moment and mass of the dark matter using Planck-2018 and BAO data.

TABLE IV. Planck-2018 and BAO constraints on magnetic dipole momentum and mass of Majorana fermion dark matter with the other six parameters of ΛCDM.

Parameter	68% limits	95% limits	99% limits
$\Omega_b h^2$	0.02244 ± 0.00013	$0.02244^{+0.00026}_{-0.00026}$	$0.02244^{+0.00034}_{-0.00034}$
$\Omega_c h^2$	0.11920 ± 0.00091	$0.1192^{+0.0018}_{-0.0018}$	$0.1192^{+0.0023}_{-0.0023}$
τ	0.0564 ± 0.0073	$0.056^{+0.015}_{-0.014}$	$0.056^{+0.020}_{-0.018}$
$\ln(10^9(\mu/\mu_B))$	$-2.0^{+4.0}_{-6.4}$	<5.69	<7.36
$\log_{10}(m_\chi/GeV)$	…	…	…
$\ln(10^{10}A_s)$	3.047 ± 0.014	$3.047^{+0.029}_{-0.028}$	$3.047^{+0.039}_{-0.037}$
n_s	0.9671 ± 0.0037	$0.9671^{+0.0073}_{-0.0072}$	$0.9671^{+0.0096}_{-0.0093}$
H_0	67.72 ± 0.41	$67.72^{+0.82}_{-0.79}$	$67.7^{+1.1}_{-1.0}$

We can see from Table III that

$$\mathcal{D} < 7.978 \times 10^{-9}\ e\,\mathrm{cm} \quad 95\%\ \mathrm{C.L.} \tag{33}$$

Table IV represents the constraints on magnetic dipole moment and mass of the dark matter obtained from Planck-2018 and BAO data. Here also we have quoted the constraints on the other six parameters of ΛCDM. Figure 3 represents the marginalized constraints on magnetic dipole moment and mass of the dark matter along with joint 68% C.L. and 95% C.L. constraints on both the parameters.

Again we can read from Table IV that

$$\mu < 2.959 \times 10^{-7}\ \mu_B \quad 95\%\ \mathrm{C.L.} \tag{34}$$

Similarly Table V lists the constraints on Rayleigh coupling and mass of the scalar dark matter. Figure 4 represents the marginalized constraints on both of these parameters along with joint 68% C.L. and 95% C.L. constraints from Planck-2018 and BAO data. Again we have mentioned constraints on the other six parameters of ΛCDM.

We can see from Table V that

$$\frac{g_4}{\Lambda_4^2} < 1.085 \times 10^{-2}\ \mathrm{GeV}^{-2} \quad 95\%\ \mathrm{C.L.} \tag{35}$$

The upper bounds given by Eqs. (32)–(35) are obtained after marginalizing over all other parameters.

V. COMPARISON WITH CONSTRAINTS FROM OTHER EXPERIMENTS

In order to obtain the correct relic density of sub-GeV dark matter we require mediators in the sub-GeV mass range [2]. We can describe dark matter interactions, where the energy transfer is so small, with effective operators like anapole, dipole and Rayleigh form factors, which are effective below the cutoff scale $\Lambda \sim$ GeV. These low energy effective form factors cannot be constrained from colliders, and the best bounds are obtained from the low energy processes like electron scattering in direct detection experiments or in searches of sub-GeV scale gamma rays from galaxies. The constraints which can be obtained on TeV scale effective theories from colliders

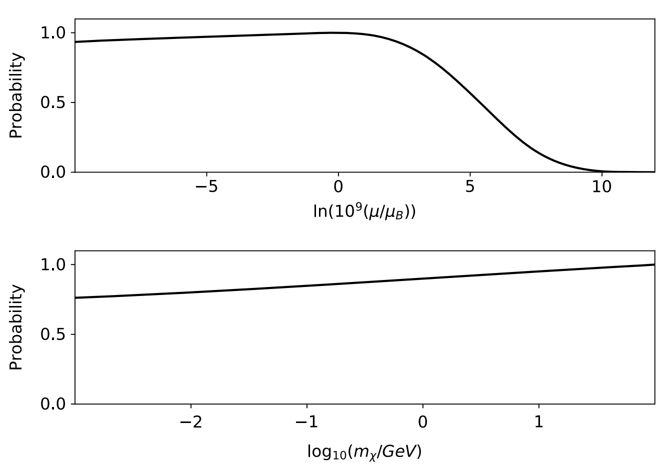

(a) Marginalized constraints

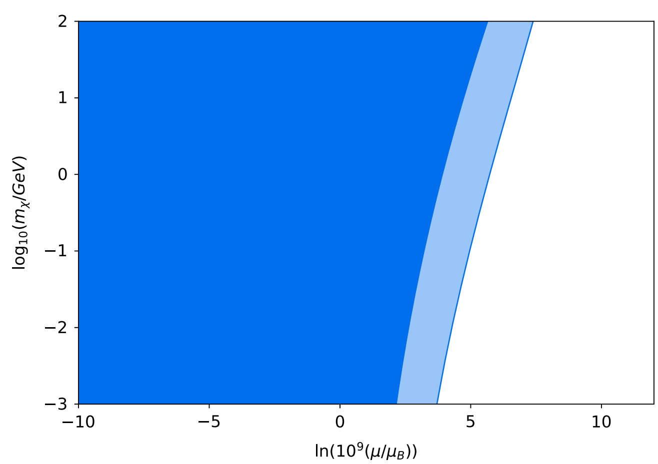

(b) Joint 68% CL and 95%CL constraints

FIG. 3. Constraints for magnetic dipole moment and mass of the dark matter using Planck-2018 and BAO data.

TABLE V. Planck-2018 and BAO constraints on Rayleigh coupling and mass of dark matter with the other six parameters of ΛCDM.

Parameter	68% limits	95% limits	99% limits
$\boldsymbol{\Omega_b h^2}$	0.02244 ± 0.00013	$0.02244^{+0.00026}_{-0.00026}$	$0.02244^{+0.00034}_{-0.00034}$
$\boldsymbol{\Omega_c h^2}$	0.11919 ± 0.00092	$0.1192^{+0.0018}_{-0.0018}$	$0.1192^{+0.0023}_{-0.0024}$
$\boldsymbol{\tau}$	0.0567 ± 0.0074	$0.057^{+0.015}_{-0.014}$	$0.057^{+0.020}_{-0.019}$
$\mathbf{ln}(10^9(g_4/\Lambda_4^2 GeV^{-2}))$	<6.43	<16.2	<19.7
$\mathbf{log_{10}}(m_\chi/GeV)$	<-3.55	...	...
$\mathbf{ln}(10^{10} A_s)$	3.048 ± 0.015	$3.048^{+0.030}_{-0.028}$	$3.048^{+0.040}_{-0.037}$
$\boldsymbol{n_s}$	0.9671 ± 0.0037	$0.9671^{+0.0073}_{-0.0073}$	$0.9671^{+0.0097}_{-0.0096}$
H_0	67.73 ± 0.41	$67.73^{+0.81}_{-0.80}$	
	$67.7^{+1.1}_{-1.1}$		

is studied in [48]. We compare the bounds from CMB distortion by dark matter annihilation obtained in this paper with the bounds on the electromagnetic form factors from other experiments and astrophysical observations in this section.

A. Electric, magnetic and anapole moments

For sub-GeV mass fermionic dark matter the best bounds come from the ionization of atoms with electron scattering process $\chi + e^- \to \chi + e^-$ in direct detection experiments like Xenon-10 [4], DarkSide [5] and Xenon-1T [6]. The most stringent bounds come from Xenon-10 [4] and Xenon-1T [6] which are dark matter mass dependent. The bound on anapole moment of Majorana dark matter is $g_A < (10^2\text{–}0.5 \times 10^{-1})$ GeV^{-2} in the mass range $m_\chi = (0.2$ MeV–1 GeV$)$ [7]. This is more stringent than the CMB bound $g_A < 7.163 \times 10^3$ GeV^{-2} (for $m_\chi \geq 0.5$ MeV) since the CMB bound is based on annihilation process $\chi\chi \to e^+e^-$, whose cross section is velocity suppressed (15).

The bound on electric dipole moment of Xenon-10 [4] and Xenon-1T [6] of Dirac dark matter with mass in the range $m_\chi = (0.2$ MeV–1 GeV$)$ is $\mathcal{D} < (6.6 \times 10^{-18}\text{–}3.9 \times 10^{-20})e$ cm [7]. This is again more stringent than the CMB bound $\mathcal{D} < 7.978 \times 10^{-9}$ e cm (for $m_\chi \geq 0.5$ MeV) as the annihilation cross section for electric dipole annihilation is velocity suppressed (21).

Finally bound on magnetic dipole moment from Xenon-10 [4] and Xenon-1T [6] of Dirac dark matter with mass in the range $m_\chi = (0.2$ MeV–1 GeV$)$ is $\mu < (1.2 \times 10^{-5}\text{–}5.9 \times 10^{-8})\mu_B$ [7]. This is comparable to the CMB bound $\mu < 2.959 \times 10^{-7}\mu_B$ (for $m_\chi \geq 0.5$ MeV). The CMB bound is comparable with the direct detection bounds as the annihilation cross section for magnetic dipole annihilation is not velocity suppressed (26).

B. Rayleigh form factor of scalar dark matter

Constraints on the Rayleigh form factor (4) are obtained from electron ionization by Xenon-1T [6] and by searches for γ ray line spectrum in the Milky Way center by Fermi-LAT [31]. For dark matter of mass ~GeV the bound from the Fermi-LAT search is $g_4/\Lambda_4^2 < 10^{-3}$ GeV^{-2}, and from Xenon-1T the bound is $g_4/\Lambda_4^2 < 0.25$ GeV^{-2} [17].

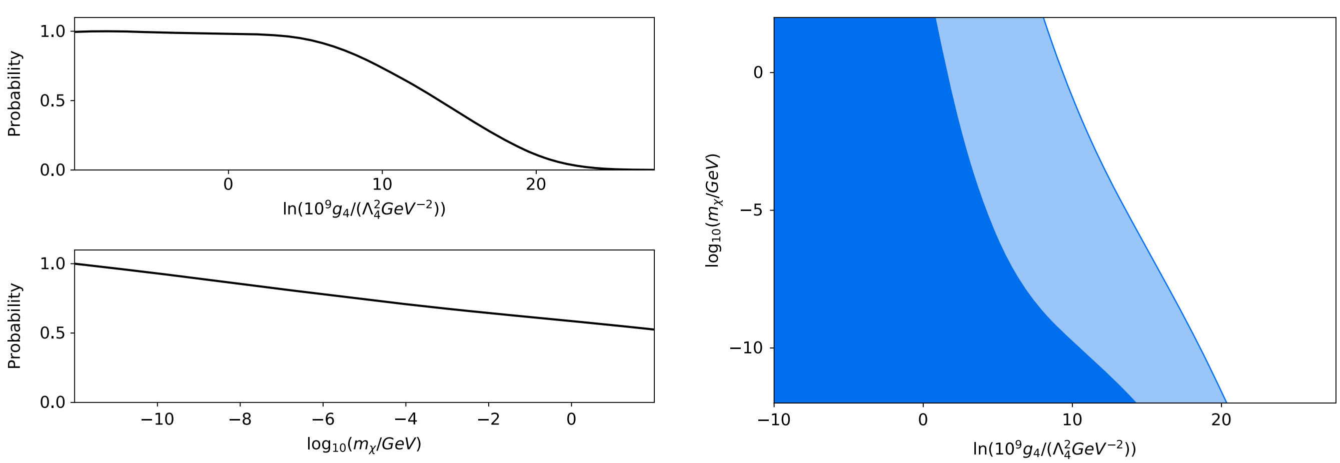

(a) Marginalized constraints (b) Joint 68% CL and 95%CL constraints

FIG. 4. Constraints on Rayleigh coupling and mass of scalar dark matter using Planck-2018 and BAO data.

The CMB bound obtained in the paper $g_4^2/\Lambda_4^2 < 1.1 \times 10^{-2}\ \mathrm{GeV}^{-2}$ is weaker than the Fermi-LAT bound but is valid for a larger range of dark matter masses up to $m_\phi \geq \mathrm{eV}$.

VI. CONCLUSIONS

Electromagnetic form factors are an important class of interactions in the effective theories framework of classifying dark matter interactions. Dirac fermion dark matter with nonzero electric and magnetic dipole moments can give the correct relic density $\Omega_m h^2 = 0.11$ by the $\chi\chi \leftrightarrow f\bar{f}$ freeze-out process if $\mathcal{D} = 2.5 \times 10^{-16}\ e\,\mathrm{cm}$ and $\mu = 8.2 \times 10^{-7}\mu_B$ respectively [11]. Majorana fermions with anapole moment of mass 10 MeV with anapole moment $g_A = 0.11\ \mathrm{GeV}^{-2}$ can be dark matter with the correct freeze-out relic density [12].

Electromagnetic dark matter can be observed not only via electron scattering direct detection experiments [3–8] but can also be constrained from the CMB.

In this paper we have considered anapole and dipolar dark matter with masses $m_\chi > \mathcal{O}$ (MeV). We find that dark matter with electromagnetic dipole or anapole form factors will distort the CMB during the recombination era by producing relativistic electrons via the process $\chi\chi \to e^+e^-$. We find that the Planck data gives the bounds on electromagnetic form factors $\mathcal{D} < 7.978 \times 10^{-9}\ e\,\mathrm{cm}$ and $\mu < 2.959 \times 10^{-7}\ \mu_B$, and $g_A < 7.163 \times 10^3\ \mathrm{GeV}^{-2}$.

Dark matter with $\mathcal{O}(\mathrm{MeV})$ mass in thermal equilibrium with radiation will be ruled out by Big Bang Nucleosynthesis (BBN) constraints on N_{eff}. These can only be created after the BBN era by the freeze-in mechanism. Freeze-in requires very small couplings and our bounds on electric dipole and anapole moments also rule out the freeze-out mechanism for relic density. These may be produced by the freeze-in mechanism which requires smaller couplings [2,49].

For scalar dark matter there is the dimension-6 Rayleigh operator coupling with photons. We put the bound on the Rayleigh coupling as $\frac{g_4}{\Lambda_4^2} < 1.085 \times 10^{-2}\ \mathrm{GeV}^{-2}$ (95% C.L.). This bound is valid for dark matter mass as low as $\mathcal{O}(\mathrm{eV})$. Such light dark matter can only be produced by the freeze-in mechanism to evade bounds from BBN.

Spectral distortion of the CMB can also arise from radiatively decaying dark matter [50]. The bounds derived on the radiative lifetime can be used for deriving bounds on dipolar couplings of Majorana dark matter which can have nonzero transition electric and magnetic moments dipole.

ACKNOWLEDGMENTS

A. N. would like to thank the Indian Space Research Organization, Department of Space, Government of India, for providing financial support via the RESPOND program Grant No. DS_2B-13012(2)/47/2018-Sec. II.

[1] T. Marrodán Undagoitia and L. Rauch, Dark matter direct-detection experiments, J. Phys. G **43**, 013001 (2016).
[2] S. Mohanty, Astroparticle physics and cosmology: Perspectives in the multimessenger era, Lect. Notes Phys. **975**, 1 (2020).
[3] R. Essig, J. Mardon, and T. Volansky, Direct detection of sub-GeV dark matter, Phys. Rev. D **85**, 076007 (2012).
[4] R. Essig, A. Manalaysay, J. Mardon, P. Sorensen, and T. Volansky, First Direct Detection Limits on sub-GeV Dark Matter from XENON10, Phys. Rev. Lett. **109**, 021301 (2012).
[5] P. Agnes *et al.* (DarkSide Collaboration), Constraints on Sub-GeV Dark-Matter–Electron Scattering from the DarkSide-50 Experiment, Phys. Rev. Lett. **121**, 111303 (2018).
[6] E. Aprile *et al.* (XENON Collaboration), Light Dark Matter Search with Ionization Signals in XENON1T, Phys. Rev. Lett. **123**, 251801 (2019).
[7] R. Catena, T. Emken, N. A. Spaldin, and W. Tarantino, Atomic responses to general dark matter-electron interactions, Phys. Rev. Research **2**, 033195 (2020).
[8] R. Catena, T. Emken, and J. Ravanis, Rejecting the Majorana nature of dark matter with electron scattering experiments, J. Cosmol. Astropart. Phys. 06 (2020) 056.
[9] M. Pospelov and T. ter Veldhuis, Direct and indirect limits on the electromagnetic form-factors of WIMPs, Phys. Lett. B **480**, 181 (2000).
[10] K. Sigurdson, M. Doran, A. Kurylov, R. R. Caldwell, and M. Kamionkowski, Dark-matter electric and magnetic dipole moments, Phys. Rev. D **70**, 083501 (2004); Erratum, Phys. Rev. D **73**, 089903 (2006).
[11] E. Masso, S. Mohanty, and S. Rao, Dipolar dark matter, Phys. Rev. D **80**, 036009 (2009).
[12] C. M. Ho and R. J. Scherrer, Anapole dark matter, Phys. Lett. B **722**, 341 (2013).
[13] E. Del Nobile, G. B. Gelmini, P. Gondolo, and J. H. Huh, Direct detection of light anapole and magnetic dipole DM, J. Cosmol. Astropart. Phys. 06 (2014) 002.
[14] R. Primulando, E. Salvioni, and Y. Tsai, The dark penguin shines light at colliders, J. High Energy Phys. 07 (2015) 031.
[15] A. De Simone and T. Jacques, Simplified models vs effective field theory approaches in dark matter searches, Eur. Phys. J. C **76**, 367 (2016).
[16] X. Chu, J. Pradler, and L. Semmelrock, Light dark states with electromagnetic form factors, Phys. Rev. D **99**, 015040 (2019).

[17] B. J. Kavanagh, P. Panci, and R. Ziegler, Faint light from dark matter: Classifying and constraining dark matter-photon effective operators. J. High Energy Phys. 04 (2019) 089.
[18] J. Kopp, L. Michaels, and J. Smirnov, Loopy constraints on leptophilic dark matter and internal bremsstrahlung, J. Cosmol. Astropart. Phys. 04 (2014) 022.
[19] C. M. Ho and R. J. Scherrer, Sterile neutrinos and light dark matter save each other, Phys. Rev. D **87**, 065016 (2013).
[20] C. Boehm, M. J. Dolan, and C. McCabe, A lower bound on the mass of cold thermal dark matter from Planck, J. Cosmol. Astropart. Phys. 08 (2013) 041.
[21] C. Brust, D. E. Kaplan, and M. T. Walters, New light species and the CMB, J. High Energy Phys. 12 (2013) 058.
[22] X. L. Chen and M. Kamionkowski, Particle decays during the cosmic dark ages, Phys. Rev. D **70**, 043502 (2004).
[23] N. Padmanabhan and D. P. Finkbeiner, Detecting dark matter annihilation with CMB polarization: Signatures and experimental prospects, Phys. Rev. D **72**, 023508 (2005).
[24] S. Galli, F. Iocco, G. Bertone, and A. Melchiorri, CMB constraints on dark matter models with large annihilation cross section, Phys. Rev. D **80**, 023505 (2009).
[25] T. R. Slatyer, N. Padmanabhan, and D. P. Finkbeiner, CMB constraints on WIMP annihilation: Energy absorption during the recombination epoch, Phys. Rev. D **80**, 043526 (2009).
[26] D. P. Finkbeiner, S. Galli, T. Lin, and T. R. Slatyer, Searching for dark matter in the CMB: A compact parametrization of energy injection from new physics, Phys. Rev. D **85**, 043522 (2012).
[27] N. Aghanim *et al.* (Planck Collaboration), Planck 2018 results. VI. Cosmological parameters, Astron. Astrophys. **641**, A6 (2020).
[28] J. Cang, Y. Gao, and Y. Z. Ma, Probing dark matter with future CMB measurements, Phys. Rev. D **102**, 103005 (2020).
[29] C. Arellano-Celiz, A. Avilez-López, J. E. Barradas-Guevara, and O. Félix-Beltrán, Annihilation of dipolar dark matter to photons, arXiv:1908.05695.
[30] A. Albert *et al.* (Fermi-LAT and DES Collaborations), Searching for dark matter annihilation in recently discovered Milky Way satellites with FERMI-LAT, Astrophys. J. **834**, 110 (2017).
[31] M. Ackermann *et al.* (Fermi-LAT Collaboration), Updated search for spectral lines from Galactic dark matter interactions with pass 8 data from the Fermi Large Area Telescope, Phys. Rev. D **91**, 122002 (2015).
[32] P. J. E. Peebles, Recombination of the primeval plasma, Astrophys. J. **153**, 1 (1968).
[33] Y. B. Zeldovich, V. G. Kurt, and R. A. Sunyaev, Recombination of hydrogen in the hot model of the universe, Zh. Eksp. Teor. Fiz. **55**, 278 (1968) [J. Exp. Theor. Phys. **28**, 146 (1969)].
[34] S. Seager, D. D. Sasselov, and D. Scott, How exactly did the universe become neutral?, Astrophys. J. Suppl. Ser. **128**, 407 (2000).
[35] G. Huetsi, A. Hektor, and M. Raidal, Constraints on leptonically annihilating dark matter from reionization and extragalactic gamma background, Astron. Astrophys. **505**, 999 (2009).
[36] C. Evoli, S. Pandolfi, and A. Ferrara, CMB constraints on light dark matter candidates, Mon. Not. R. Astron. Soc. **433**, 1736 (2013).
[37] S. Galli, T. R. Slatyer, M. Valdes, and F. Iocco, Systematic uncertainties in constraining dark matter annihilation from the cosmic microwave background, Phys. Rev. D **88**, 063502 (2013).
[38] M. S. Madhavacheril, N. Sehgal, and T. R. Slatyer, Current dark matter annihilation constraints from CMB and low-redshift data, Phys. Rev. D **89**, 103508 (2014).
[39] S. Galli, F. Iocco, G. Bertone, and A. Melchiorri, Updated CMB constraints on dark matter annihilation cross sections, Phys. Rev. D **84**, 027302 (2011).
[40] G. Giesen, J. Lesgourgues, B. Audren, and Y. Ali-Haimoud, CMB photons shedding light on dark matter, J. Cosmol. Astropart. Phys. 12 (2012) 008.
[41] L. Zhang, X. L. Chen, Y. A. Lei, and Z. G. Si, The impacts of dark matter particle annihilation on recombination and the anisotropies of the cosmic microwave background, Phys. Rev. D **74**, 103519 (2006).
[42] L. Zhang, X. Chen, M. Kamionkowski, Z. g. Si, and Z. Zheng, Constraints on radiative dark-matter decay from the cosmic microwave background, Phys. Rev. D **76**, 061301 (2007).
[43] A. Lewis, A. Challinor, and A. Lasenby, Efficient computation of CMB anisotropies in closed FRW models, Astrophys. J. **538**, 473 (2000).
[44] J. Chluba and R. M. Thomas, Towards a complete treatment of the cosmological recombination problem, Mon. Not. R. Astron. Soc. **412**, 748 (2011).
[45] Y. Ali-Haimoud and C. M. Hirata, HyRec: A fast and highly accurate primordial hydrogen and helium recombination code, Phys. Rev. D **83**, 043513 (2011).
[46] A. Lewis and S. Bridle, Cosmological parameters from CMB and other data: A Monte Carlo approach, Phys. Rev. D **66**, 103511 (2002).
[47] P. A. R. Ade *et al.* (Planck Collaboration), Planck 2013 results. XVI. Cosmological parameters, Astron. Astrophys. **571**, A16 (2014).
[48] C. Arina, A. Cheek, K. Mimasu, and L. Pagani, Light and darkness: Consistently coupling dark matter to photons via effective operators, Eur. Phys. J. C **81**, 223 (2021).
[49] L. J. Hall, K. Jedamzik, J. March-Russell, and S. M. West, Freeze-in production of FIMP dark matter, J. High Energy Phys. 03 (2010) 080.
[50] B. Bolliet, J. Chluba, and R. Battye, Spectral distortion constraints on photon injection from low-mass decaying particles, arXiv:2012.07292.